

1 **Electronic Supplementary Information**

2 **for**

3 **Linking microscopic structural changes and macroscopic mechanical responses**

4 **in a near-ideal bottlebrush elastomer under uniaxial deformation**

5

6 **Authors:**

7 Shintaro Nakagawa<sup>1\*</sup> and Naoko Yoshie<sup>1\*</sup>

8

9 **Affiliations:**

10 1: Institute of Industrial Science, the University of Tokyo, Komaba 4-6-1, Meguro-ku, Tokyo 153-

11 8505 Japan

12

13 \* Corresponding author. E-mail: snaka@iis.u-tokyo.ac.jp (S.N.), yoshie@iis.u-tokyo.ac.jp (Y.N.)

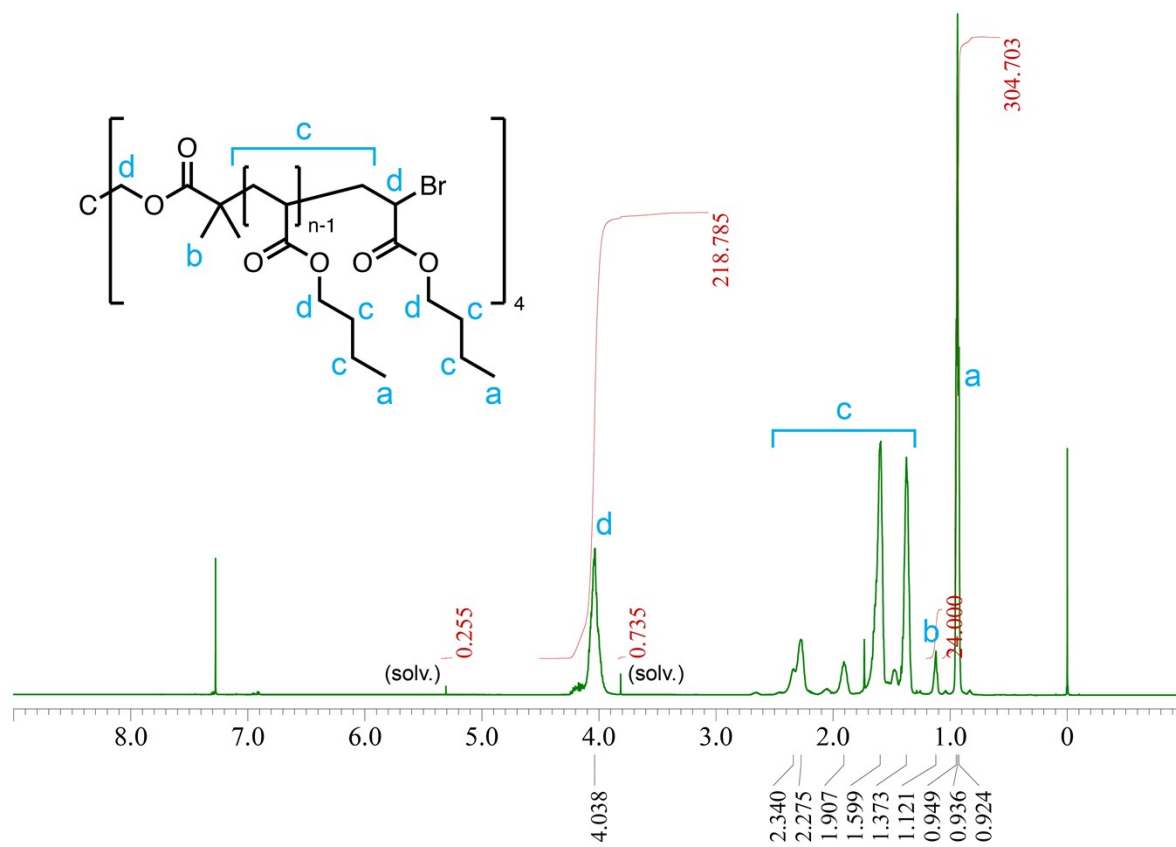
14

15

## 16 S1. Synthesis of star P*n*BA.

17 The tetrafunctional initiator, pentaerythritol tetrakis(2-bromoisobutyrate) (4f-BiB) was  
18 synthesized according to the literature procedure<sup>1</sup>. *n*-Butyl acrylate (*n*BA; FUJIFILM Wako Pure  
19 Chemical Corp., Japan) was passed through a short column of activated alumina before use. Copper(I)  
20 bromide (CuBr; FUJIFILM Wako) was purified by washing in glacial acetic acid overnight and then in  
21 ethanol and diethyl ether and vacuum drying. All other reagents were used as received. In a 200 mL  
22 Schlenk flask, 1464 mg of 4f-BiB (2.00 mmol, 1 eq.) and 51.267 g of *n*BA (400.0 mmol, 200 eq.), 57.88  
23 mg of *N,N,N',N'',N'''*-pentamethyldiethylenetriamine (PMDETA, 0.334 mmol, 0.167 eq.), and anisole  
24 16 mL were added and the mixture was degassed by three freeze-pump-thaw cycles. After the third  
25 pumping procedure, 57.00 mg of CuBr (0.3974 mmol; 0.199 eq.) was added onto the frozen solution  
26 under nitrogen flow, and the tube was evacuated once again. After melting the solution in nitrogen  
27 atmosphere, the polymerization was initiated by heating the tube in a 50 °C oil bath. The reaction was  
28 monitored by sampling the aliquots of the reaction mixture and analyzing it by <sup>1</sup>H NMR. After 5 h, the  
29 reaction was quenched by cooling in liquid nitrogen and exposing to air. The monomer conversion  
30 estimated from the <sup>1</sup>H NMR of the quenched reaction mixture was 46%. The solution was precipitated  
31 in 8:2 methanol/water mixture three times. The viscous polymer was dissolved in DCM and washed  
32 with water twice. After concentrating the DCM solution in air, the solution was precipitated in 8:2  
33 methanol/water mixture twice, and the liquid polymer was washed with water two more times. The  
34 polymer was dissolved in DCM and passed through a cotton puff to remove dusts and then concentrated  
35 by a rotavapor. After drying in vacuo at r.t. for ~ 2 days, the polymer was obtained as slightly green  
36 clear viscous liquid. Yield = 23.8 g (45%). The <sup>1</sup>H NMR spectrum is shown in Fig. S1.  $M_n = 13.8$  kDa.  
37 Size-exclusion chromatography (light scattering detector):  $M_n = 13.1$  kDa,  $M_w/M_n = 1.06$ .

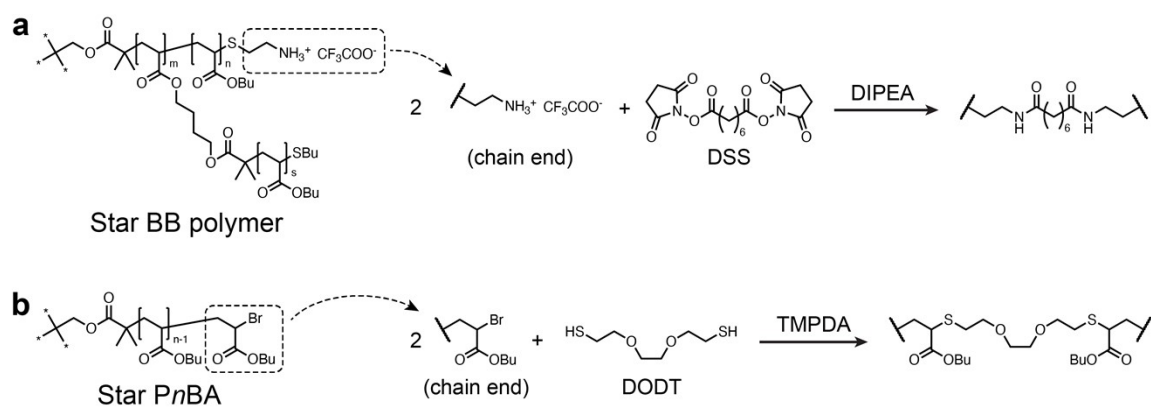
38



39

40 Fig. S1. The <sup>1</sup>H NMR spectrum of star PnBA in CDCl<sub>3</sub>.

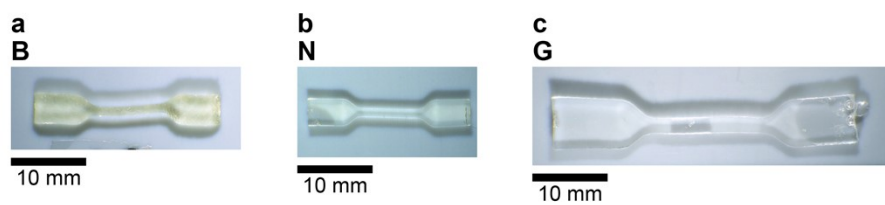
41



42

43 Fig. S2. Reactions scheme of the synthesis of (a) **B** and (b) **N**.

44



45

46 Fig. S3. Photographs of the test pieces of (a) **B**, (b) **N**, and (c) **G**.



47

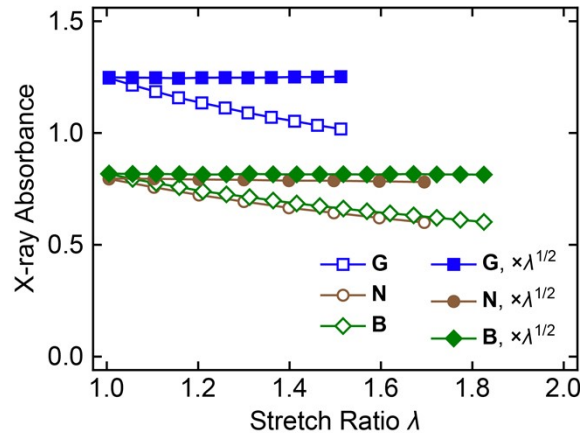
48 Fig. S4. Photographs of the tensile-SAXS set-up.

49

50

51 **S2. Verification of normal incidence geometry and sample incompressibility from X-ray**  
 52 **absorbance in tensile-SAXS.**

53 Fig. S5 (open symbols) plots the X-ray absorbance ( $A = -\ln \tau$  where  $\tau$  is the transmittance)  
 54 against stretch ratio ( $\lambda$ ) for the three network samples.  $A$  decreases with increasing  $\lambda$  due to thinning by  
 55 stretching. For a normal incidence geometry,  $A$  obeys a Beer-Lambert law  $A = \mu l$  where  $\mu$  is the linear  
 56 absorption coefficient and  $l$  is the sample thickness.  $\mu$  usually depends solely on the atomic composition  
 57 and the physical density and hence is invariant against stretching provided that the material is  
 58 incompressible. Incompressibility also leads to  $l \propto \lambda^{-1/2}$ . Therefore,  $A\lambda^{1/2}$  should be constant  
 59 independent of  $\lambda$ . The results of such correction are plotted in closed symbols in Fig. S5, indeed showing  
 60 independence on  $\lambda$ . Therefore, the normal incidence of the X-ray beam and the incompressibility of the  
 61 samples are verified. The result further suggests that  $l$ , which is required for thickness correction in  
 62 SAXS data reduction, is obtained simply as  $l = l_0 \lambda^{-1/2}$  where  $l_0$  is the thickness before stretching. The  
 63 scattered intensity reported in the present paper has been corrected for the thickness estimated by this  
 64 method.



65  
 66 Fig. S5. X-ray absorbance during uniaxial tensile tests. Open symbols are the observed absorbance and  
 67 close symbols are the absorbance corrected for the expected thickness reduction by stretching an  
 68 incompressible material.

69  
 70

71 **S3. Polarization correction in SAXS.**

72 The scattered intensity  $I_{obs}$  from an isotropic material shows anisotropic scattered intensity if  
73 the beam is polarized and is described as<sup>2</sup>

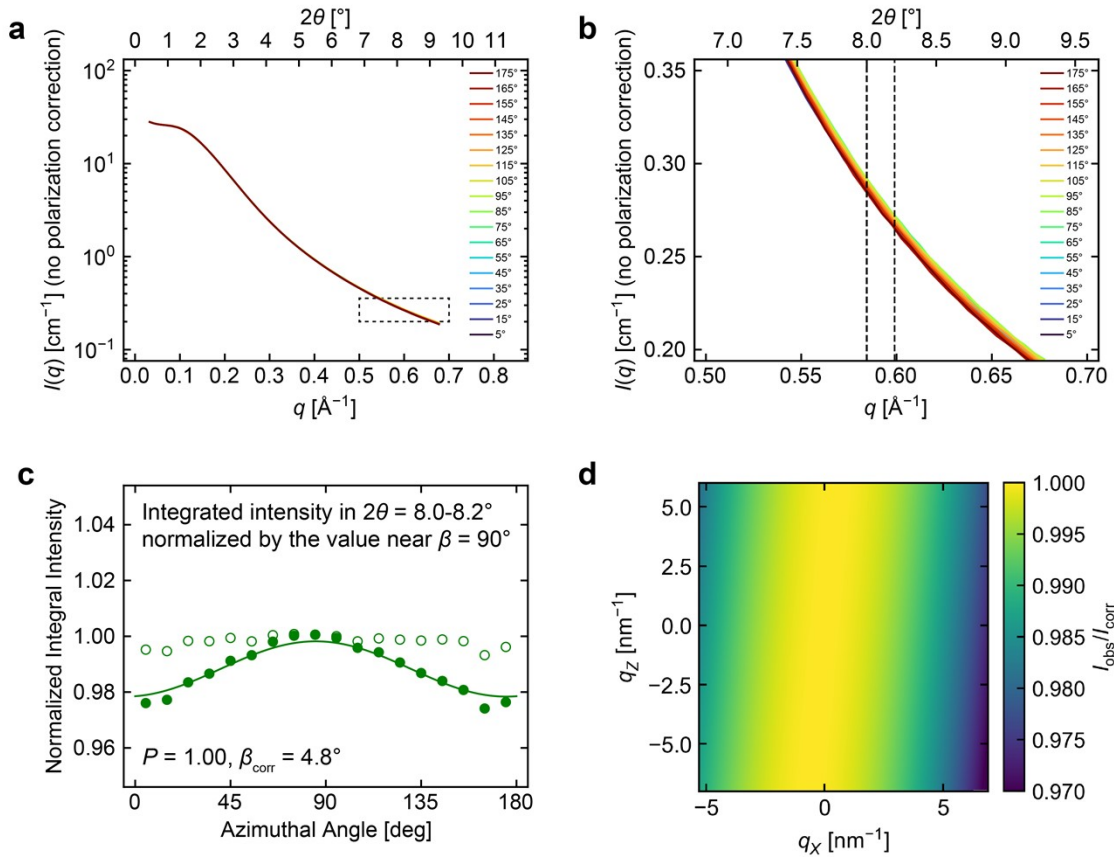
$$74 \quad I_{obs} = I_{corr} [P(1 - \cos^2 \beta \sin^2 2\theta) + (1 - P)(1 - \sin^2 \beta \sin^2 2\theta)] \quad (S1)$$

75 where  $I_{corr}$  is the intensity expected when the polarization effect is absent,  $P$  is the fraction of the  
76 horizontally polarized component of the incident beam, and  $\beta$  is the azimuthal angle of the scattered X-  
77 ray with  $\beta = 0$  being the horizontal direction. The two terms of Equation S1, each of which represent  
78 the contribution from the horizontally and vertically polarized components in incident beam, can be  
79 obtained by letting  $I' = 1$  (horizontal polarization) and  $-1$  (vertical polarization) in Equation 12 in ref.  
80 2, respectively. The equation means that a horizontally polarized incident beam ( $P > 0.5$ ) leads to  
81 reduction of the scattered intensity along the equator ( $\beta = 0^\circ$  and  $180^\circ$ ). Fig. S6a shows the sector  
82 averaged 1D profiles of scattered intensity from an isotropic glassy carbon standard (SRM3600, NIST,  
83 USA) collected by using the same setup used for the tensile-SAXS measurements. Close examination  
84 of the profiles at the high  $q$  region (Fig. S6b) reveals slight reduction at around  $\beta = 0^\circ$  and  $180^\circ$ ,  
85 indicating that the incident beam is horizontally polarized. To quantify the extent and the direction of  
86 polarization, the intensity in the range  $8.0^\circ \leq 2\theta \leq 8.2^\circ$  was integrated to get the azimuthal intensity  
87 profile (Fig. S6c, closed symbols). The azimuthal profile was then fitted with the slightly modified  
88 equation.

$$89 \quad I_{obs} = I_{corr} [P(1 - \cos^2 (\beta + \beta_{corr}) \sin^2 2\theta) + (1 - P)(1 - \sin^2 (\beta + \beta_{corr}) \sin^2 2\theta)] \quad (S2)$$

90 where  $\beta_{corr}$  accounts for a slight tilt of the polarization axis. The fitting result is shown in Fig. S6c as a  
91 solid curve. The optimized parameters are  $P = 1.00$  and  $\beta_{corr} = 4.8^\circ$ . The azimuthal profile after  
92 correction by Equation S2 using the optimized parameters is shown as open symbols in Fig. S6c, in  
93 which an isotropic intensity distribution is seen. Fig. S6d shows the 2D plot of  $I_{obs}/I_{corr}$  calculated by  
94 using Equation S2 with the above optimized  $P$  and  $\beta_{corr}$  values. The polarization correction was  
95 performed by dividing the observed intensity by the values in Fig. S6d. The scattered intensities  
96 reported in the main text (Fig. 3-6) are those after the correction.

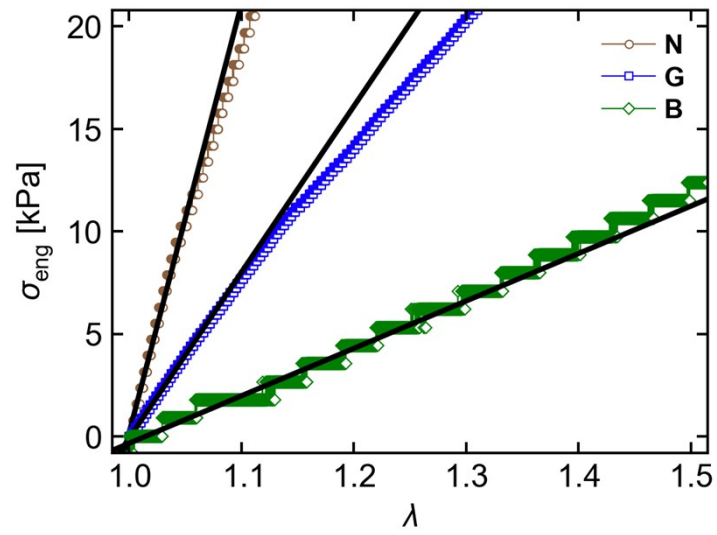
97



98

99 Fig. S6. (a) 1D profiles of the scattered intensity from an isotropic glassy carbon sample at each  
 100 azimuthal angle  $\beta$  indicated. (b) Enlarged graph showing the region marked by dashed lines in panel a.  
 101 (c) Azimuthal intensity profile (closed symbol) obtained by integrating the intensity in the region  
 102 marked by dashed vertical lines in panel b. The integrated intensity has been normalized by the  
 103 maximum value. The solid curve is the fitting result using Equation S2. Open symbols show the result  
 104 of the polarization correction. (d) 2D plot of the polarization factor calculated by using Equation S2  
 105 with the optimized parameters ( $P = 1.00$  and  $\beta_{\text{corr}} = 4.8^\circ$ ). The values lower than unity show the effect  
 106 of the polarized incident beam.

107



108

109 Fig. S7. Results of linear fitting to obtain Young's modulus ( $E_Y$ ). Black solid lines indicate the fitted  
110 lines.

111



#### 112 S4. Estimation of the diameter of BB polymer and PnBA.

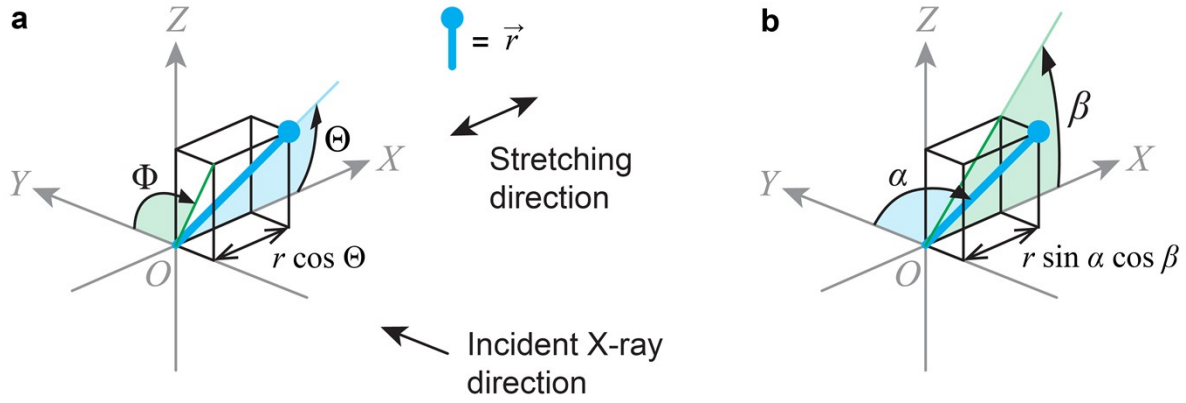
113 The volume of a repeat unit ( $v_u$ ) of PnBA ( $0.128 \text{ kg mol}^{-1}$ ) is calculated to be  $0.20 \text{ nm}^3$  using  
114 the physical density of PnBA ( $1090 \text{ kg m}^{-3}$ ). The length of a fully extended PnBA chain per repeat  
115 unit ( $l_u$ ) is roughly  $2l_b \sin(\theta_b/2)$  where  $l_b$  is the backbone bond length and  $\theta_b$  is the bond angle. We  
116 assume standard C-C bond length  $l_b = 0.154 \text{ nm}$  and the tetrahedral angle  $\cos(\theta_b) = -1/3$  (  
117  $\sin(\theta_b/2) = (2/3)^{1/2}$ ), leading to  $l_u = 0.25 \text{ nm}$ . If a PnBA chain is seen as a simple cylinder, its cross  
118 section is  $v_u/l_u = 0.20 \text{ nm}^3/0.25 \text{ nm} = 0.80 \text{ nm}^2$  which then lead to the diameter of  $\sim 1.0 \text{ nm}$ .

119 The star BB polymer had  $M_n = 86.7 \text{ kDa}$ . The molar mass of one arm is  $86.7/4 = 21.7 \text{ kDa}$ .  
120 Assuming that the star polymer in the melt state has the physical density identical to that of PnBA ( $1090$   
121  $\text{ kg m}^{-3}$ ), the volume of one arm is  $21.7/1090/N_A = 33 \text{ nm}^3$ . The polymerization degree of the backbone  
122 per one arm is 9.3 (polymerization degree of the part of the backbone chain grafted with the side chains),  
123 and its fully extended length is roughly  $9.3 \times 2 \times l_u = 2.3 \text{ nm}$  using the same assumption and the  $l_u$  value  
124 in the previous paragraph. Considering an arm as a simple cylinder, its cross section is  $33 \text{ nm}^3/2.3 \text{ nm}$   
125  $= 14 \text{ nm}^2$ , leading to the diameter of  $4.2 \text{ nm}$ .

126

127

128 **S5. Orientation parameter.**



129

130 Fig. S8. Geometry for discussion of pole orientation. (a) Definition of the polar coordinate  $O-r\theta\Phi$ . (b)

131 Definition of the polar coordinate  $O-r\alpha\beta$ .

132

133 Suppose a distribution of poles  $D(\vec{r})$  in a Cartesian coordinate  $O-XYZ$ . The number of poles in  
 134 a volume element at  $\vec{r}$  is  $D(\vec{r})d\vec{r}$ . We set the stretching direction parallel to the  $X$  axis. For the sample  
 135 being stretched,  $D(\vec{r})$  is axisymmetric around the  $X$  axis and mirror-symmetric about the  $YZ$  plane. Thus  
 136  $D(\vec{r})$  is conveniently written in a spherical coordinate  $O-r\theta\Phi$  where  $r$  is the distance from the origin,  
 137  $\theta$  is the angle from the symmetry axis, and  $\Phi$  is the azimuthal angle in the  $YZ$  plane, as depicted in Fig.  
 138 S8a. The number of poles in a volume element defined by the intervals  $[r, r + dr]$ ,  $[\theta, \theta + d\theta]$ , and  
 139  $[\Phi, \Phi + d\Phi]$  is  $D(r, \theta, \Phi)r^2 \sin \theta dr d\theta d\Phi$ . From the symmetry  $D(\vec{r})$  is independent on  $\Phi$ . Furthermore, by  
 140 focusing only on the poles with a prescribed length  $r_0$ , the  $r$ -dependence is represented by a Dirac delta  
 141 function  $\delta(r - r_0)$ :

142 
$$D(r, \theta, \Phi) = D(\theta)\delta(r - r_0) \quad (S3)$$

143 The orientation of the pole, with respect to the symmetry axis, is often measured by the average of  
 144  $\cos^2 \theta$ ,  $\langle \cos^2 \theta \rangle$ .

$$\begin{aligned}
\langle \cos^2 \theta \rangle &= \frac{\int_0^\infty dr \int_0^\pi d\theta \int_0^{2\pi} d\Phi [\cos^2 \theta D(\theta) \delta(r - r_0) \sin \theta]}{\int_0^\infty dr \int_0^\pi d\theta \int_0^{2\pi} d\Phi [D(\theta) \delta(r - r_0) \sin \theta]} \\
&= \frac{\int_0^\pi d\theta [\cos^2 \theta D(\theta) \sin \theta]}{\int_0^\pi d\theta [D(\theta) \sin \theta]} \quad (S4)
\end{aligned}$$

145

146 The explicit form of  $D(\theta)$  is usually unknown, but it may be expanded as a spherical harmonic series<sup>4</sup>.

147 For a low orientation degree, it may suffice to use the zeroth and second order terms only, which are

148 proportional to the associated Legendre polynomials of  $\cos \theta$ .

$$P_0(\cos \theta) = 1 \quad (S5)$$

$$P_2(\cos \theta) = \frac{1}{2}(3\cos^2 \theta - 1) \quad (S6)$$

149

150 Linear combination of these two terms simplifies to

$$D(\theta) = a_0 + a_2 \cos^2 \theta \quad (S7)$$

151

152 where  $a_0$  and  $a_2$  are some real coefficients. Let us evaluate  $\langle \cos^2 \theta \rangle$  for this pole distribution. The

153 normalization factor is

$$\int_0^\pi d\theta [D(\theta) \sin \theta] = \int_0^\pi d\theta [(a_0 + a_2 \cos^2 \theta) \sin \theta] = 2a_0 + \frac{2}{3}a_2 \quad (S8)$$

154

155 The numerator is

$$\begin{aligned}
\int_0^\pi d\theta [\cos^2 \theta D(\theta) \sin \theta] &= a_0 \int_0^\pi d\theta [\cos^2 \theta \sin \theta] + a_2 \int_0^\pi d\theta [\cos^4 \theta \sin \theta] \\
&= \frac{2}{3}a_0 + \frac{2}{5}a_2 \quad (S9)
\end{aligned}$$

156

157 Combining Equations S8 and S9 into S4,

$$\langle \cos^2 \theta \rangle = \frac{5a_0 + 3a_2}{15a_0 + 5a_2} \quad (S10)$$

158

159  $\langle \cos^2 \theta \rangle$  becomes 1/3 for  $a_2 = 0$  (isotropic, no preferential orientation), as expected. Hermann's

160 orientation parameter ( $f$ ) is further calculated as

$$f = P_2(\langle \cos \theta \rangle) = \frac{1}{2}(3\langle \cos^2 \theta \rangle - 1) = \frac{1}{2}\left(\frac{15a_0 + 9a_2}{15a_0 + 5a_2} - 1\right) = \frac{2a_2}{15a_0 + 5a_2} \quad (S11)$$

161

162 Note that Equation S11 may be used only for a moderate degree of orientation.

163

Next, we relate the pole distribution to the observed scattered intensity. The scattered intensity at the scattering vector  $\vec{q}$  is proportional to the pole distribution function at  $\vec{q}$ . Suppose that the incident X-ray points in +Y direction and the scattered X-ray is observed by a two-dimensional detector parallel to XZ plane. For convenience let us define another coordinate  $O-r\alpha\beta$  as in Fig. S8b. In this way, the azimuthal angle ( $\beta$ ) matches the azimuthal angle on the detector plane. The angle from the +Y axis ( $\alpha$ ) is related to the scattering angle  $2\theta$  as  $\alpha = \pi/2 + \theta$ . It is easily found from Fig. S8 that  $\cos \theta = \sin \alpha \cos \beta$ . Thus  $D(\theta)$  is rewritten as

166

$$D(\alpha, \beta) = a_0 + a_2 \sin^2 \alpha \cos^2 \beta \quad (S12)$$

170

For small angle scattering,  $\theta \ll \pi/2$  so  $\alpha \approx \pi/2$  and  $\sin^2 \alpha \approx 1$ . Therefore, we can fit the observed azimuthal intensity profile with

172

$$I(\beta) = a_0 + a_2 \cos^2 \beta \quad (S13)$$

173

and insert the optimized coefficients to Equation S11 to evaluate the orientation function.

174

## 176 References

- 177 1 S. Honda and T. Toyota, Photo-triggered solvent-free metamorphosis of polymeric materials, *Nature*
- 178 *Communications*, 2017, **8**, 502.
- 179 2 R. Kahn, R. Fourme, A. Gadet, J. Janin, C. Dumas and D. André, Macromolecular crystallography
- 180 with synchrotron radiation: photographic data collection and polarization correction, *Journal of*
- 181 *Applied Crystallography*, 1982, **15**, 330–337.
- 182 3 E. Eghbali, O. Colombani, M. Drechsler, A. H. E. Müller and H. Hoffmann, Rheology and Phase
- 183 Behavior of Poly(n-butyl acrylate)-block-poly(acrylic acid) in Aqueous Solution, *Langmuir*, 2006,
- 184 **22**, 4766–4776.
- 185 4 G. R. Mitchell, A wide-angle X-ray study of the development of molecular orientation in crosslinked
- 186 natural rubber, *Polymer*, 1984, **25**, 1562–1572.

187